

Division versus Fusion: Dnm1p and Fzo1p Antagonistically Regulate Mitochondrial Shape

Hiromi Sesaki and Robert E. Jensen

Department of Cell Biology and Anatomy, The Johns Hopkins University School of Medicine, Baltimore, Maryland 21205

Abstract. In yeast, mitochondrial division and fusion are highly regulated during growth, mating and sporulation, yet the mechanisms controlling these activities are unknown. Using a novel screen, we isolated mutants in which mitochondria lose their normal structure, and instead form a large network of interconnected tubules. These mutants, which appear defective in mitochondrial division, all carried mutations in *DNM1*, a dynamin-related protein that localizes to mitochondria. We also isolated mutants containing numerous mitochondrial fragments. These mutants were defective in *FZO1*, a gene previously shown to be required for mi-

tochondrial fusion. Surprisingly, we found that in *dnm1 fzo1* double mutants, normal mitochondrial shape is restored. Induction of Dnm1p expression in *dnm1 fzo1* cells caused rapid fragmentation of mitochondria. We propose that *dnm1* mutants are defective in the mitochondrial division, an activity antagonistic to fusion. Our results thus suggest that mitochondrial shape is normally controlled by a balance between division and fusion which requires Dnm1p and Fzo1p, respectively.

Key words: mitochondrial division • mitochondrial fusion • dynamin • GTPase • yeast

MITOCHONDRIA undergo regulated fusion and division in many cell types (Bereiter-Hahn and Voth, 1994; Kawano et al., 1995), which appear to play key roles in establishing and maintaining mitochondrial shape (Tyler, 1992). In the yeast *S. cerevisiae*, mitochondria are elongated, tubule-shaped organelles that are very dynamic during growth, mating, and sporulation. Mitochondria constitutively divide and fuse during cell growth (Nunnari et al., 1997), but change their number depending on growth conditions (Stevens, 1977). During mating, mitochondria fuse immediately after cell fusion, mixing their contents, including mitochondrial DNA (mtDNA)¹ and matrix proteins (Nunnari et al., 1997; Okamoto et al., 1998). When diploids sporulate, mitochondria are dramatically reorganized moving into the four spores and surrounding each haploid nucleus (Miyakawa et al.,

1984). The yeast homologue of *fuzzy onions* (Hales and Fuller, 1997), *FZO1* was recently identified and shown to play an important role in mitochondrial fusion (Hermann et al., 1998; Rapaport et al., 1998). However, the mechanisms that control mitochondrial division are unknown.

Materials and Methods

Strain Construction

Strain YHS2, which expresses red-shifted GFP (F64L, T65C, and I167T) fused to the Cox4p presequence (residues 1-21) under the *ADHI* promoter (*ADHI-COX4-GFP*), was constructed as follows. First, pHS1 was constructed by replacing wild-type GFP in pOK29, a *HIS3-CEN* plasmid which carries *ADHI-COX4-GFP* (Kerscher, O., unpublished information), with a *NcoI*-*Bam*HI fragment carrying red-shifted GFP from pQBI25 (Quantum Biotechnologies). The *EcoRV*-*Bam*HI fragment from pHS1 was inserted into pDH9, which carries 5' and 3' untranslated regions of *MFA2* (a gift from S. Michaelis), forming pHS2. To integrate *ADHI-COX4-GFP* at chromosomal *MFA2*, a *XhoI*-*SmaI* fragment carrying 5'-*MFA2-ADHI-COX4-GFP-3'-MFA2* from pHS2 was transformed into strain SM1235, which carries *mfa2::URA3* (Michaelis and Herskowitz, 1988). Strain YHS2, which contains *MAT α mfa2::ADHI-COX4-GFP*, was selected on 5-fluoro-orotic acid medium (Adams et al., 1997). *MAT α mfa2::ADHI-COX4-GFP* strain YHS1 was obtained by crossing YHS2 to SM1227 (Michaelis and Herskowitz, 1988). Strain 1002 (*MAT α , his3, trp1, ura3, mfa2::ADHI-COX4-GFP*) was constructed by crossing YHS1 to BY4731 (Brachmann et al., 1998).

Address correspondence to Dr. Robert E. Jensen, Department of Cell Biology and Anatomy, The Johns Hopkins University School of Medicine, 725 N. Wolfe Street, Baltimore, MD 21205. Tel.: (410) 955-7291. Fax: (410) 955-4129. E-mail: rjensen@jhmi.edu

1. *Abbreviations used in this paper:* GFP, green fluorescent protein; mtDNA, mitochondrial DNA.

Mutant Isolation

YHS2 was mutagenized with 3% ethane methylsulfonate to ~30% survival (Adams et al., 1997). Mutagenized cells were suspended at $\sim 9 \times 10^5$ cells/ml on coverslips and observed using an inverted microscope and the HIQ GFP 41014 filter set (Chroma). Mutants were isolated using micropipettes (10 μ m diameter; World Precision Instruments), transferred to a drop of SD on the same coverslip, and then to YPD plates. Micropipettes were handled by an Eppendorf micromanipulator 5171.

Crosses to wild-type strain 1002 showed that all class I, II, and III mutations were recessive and caused by a defect in a single gene. Complementation tests revealed that all eight recessive class IV mutants were defective in the same gene. Crosses between class IV mutants and *TRP1* strain 194 (a gift from E. Schweizer) or *dnm1 Δ* strain JSY1361 (Otsuga et al., 1998) showed the class IV mutation was centromere linked, located on chromosome XII, and allelic to *dnm1*. *DNM1*-containing plasmid, pRU1-DNM1 (Otsuga et al., 1998), rescued the mitochondrial phenotype of all recessive class IV mutants. All dominant and semidominant class IV mutations also segregated as alleles of *dnm1*.

Gene Disruption

Complete disruptions of the *DNM1* and *FZO1* were constructed by PCR-mediated gene replacement as described (Lorenz et al., 1995) into strains BY4733 and BY4744 (Brachmann et al., 1998). For *dnm1 Δ* , we used *HIS3* plasmid pRS303 (Sikorski and Hieter, 1989) and for *fzo1 Δ* we used *kanMX4* plasmid pRS400 (Brachmann et al., 1998). MAT α *dnm1 Δ fzo1 Δ* strain YHS27 and MAT α *dnm1 Δ fzo1 Δ* strain YHS23 were constructed by crossing MAT α *dnm1 Δ* strain YHS19 to MAT α *fzo1 Δ* strain YHS22. Mitochondria in the disruption strains were visualized using pHS12, a *CEN-LEU2* plasmid containing *ADHI-COX4-GFP*. pHS12 was created by inserting the XhoI-NotI fragment from pHS1 into pRS315 (Sikorski and Hieter, 1989).

Plasmid Construction

The *DNM1* gene with a NotI site immediately preceding its termination codon was PCR amplified from yeast genomic DNA and subcloned into

pAA3, a *CEN-LEU2* plasmid which contains the HA epitope with a NotI site at its NH₂ terminus (Aiken, A., unpublished data), forming pDNM1-HA (pHS14). DNMI-GFP plasmid pHS20 was constructed as described above except that pAA1, a *CEN-LEU2* plasmid which contains GFP with a NotI site at its NH₂ terminus (Aiken, A., unpublished data), was used instead of pAA3. To form pHS15, *DNM1-HA* coding sequences were PCR amplified from pHS14 with 50 bp of flanking sequences homologous to the *GAL1-URA3* promoter in pRS314GU (Nigro et al., 1992). The *DNM1-HA* fragment and linearized pRS314GU were cotransformed into yeast and pGAL1-DNM1-HA (pHS15) was formed by homologous recombination (Oldenburg et al., 1997). pGAL1-DNM1-GFP (pHS40) was constructed as described for pHS15 except that pHS20 was used instead of pHS14.

Quantitation of Dnm1p-GFP Localization

dnm1 Δ fzo1 Δ cells carrying pGAL1-DNM1-GFP were incubated in galactose media for 1–2 h, stained with MitoTracker Red CMXRos (Molecular Probes). 12 cells were examined by fluorescence microscopy and the mitochondrially associated Dnm1p-GFP dots (82 total) were assigned to one of two locations: (a) the end of a tubule (50 dots), or (b) the side of a tubule (32 dots). The end of a tubule was defined as when the center of a Dnm1p-GFP dot was located within 0.15 μ m from the end. The average length of the mitochondrial tubules was estimated to be $2.7 \pm 1.9 \mu$ m and the diameter $\sim 0.3 \mu$ m ($n = 44$). We calculate that the side of the tubule represents 89% of the mitochondrial surface area and the remainder (11%) represents the end.

Results and Discussion

We screened for yeast mutants defective in mitochondrial shape using a novel strategy in which mitochondria are visualized by the green fluorescent protein (GFP) and mutants were isolated by micromanipulation. GFP was fused

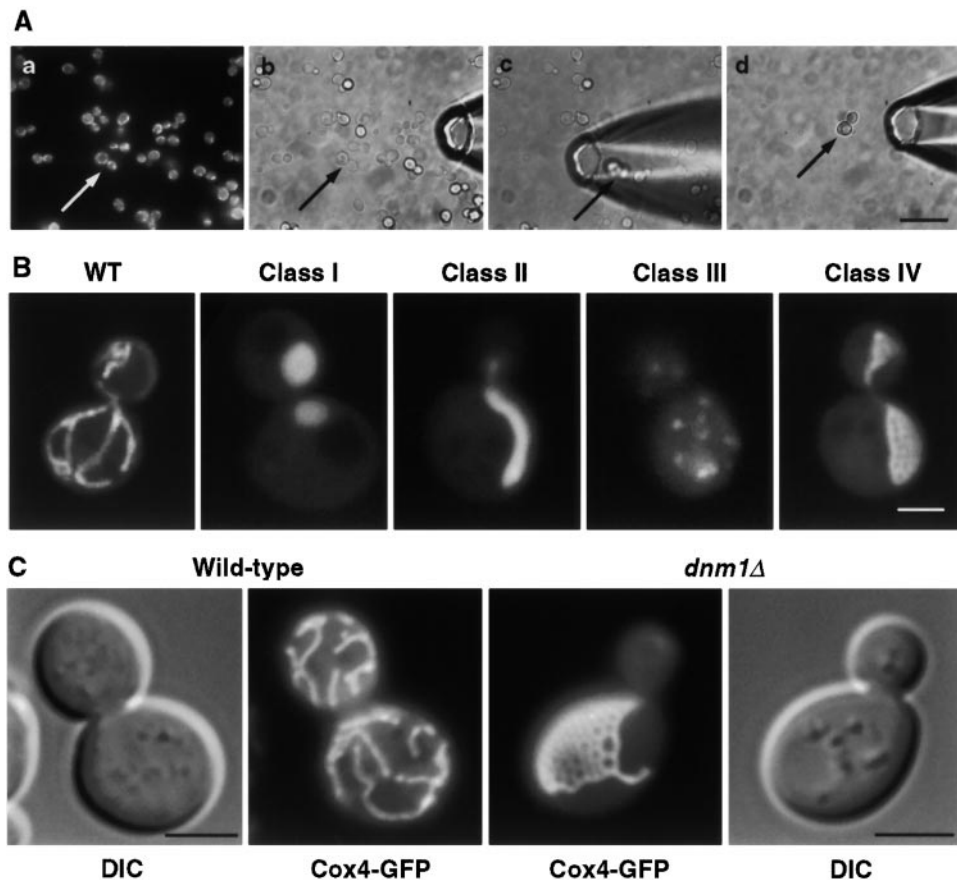


Figure 1. Mutants defective in mitochondrial shape. (A) Screen to isolate mutants defective in mitochondrial morphology. (a) Mitochondria were visualized by COX4-GFP. (b–d) Individual mutants were isolated using a micropipette. The arrow indicates a potential mutant cell. (B) Wild-type YHS2 and a representative from each class of mutants were grown in YPD to log phase and then stained with 1 μ g/ml 3,3'-dihexyloxycarbocyanine (DiOC₆) (Molecular Probes) to enhance mitochondrial fluorescence. Confocal images of cells are shown. (C) *dnm1 Δ* cells contain an interconnected network of mitochondria. Wild-type (BY4733) and isogenic *dnm1 Δ* cells expressing COX4-GFP (pHS12), were grown in YPGal to log phase. Fluorescence (COX4-GFP) and differential interference contrast (DIC) images are shown. Bars: (A) 10 μ m; (B) 2 μ m; (C) 3 μ m.

to the presequence (residues 1–21) of mitochondrial cytochrome oxidase subunit IV (COX4; Pon and Schatz, 1991). When expressed in yeast, COX4-GFP targets the mitochondrial matrix, and mitochondria were visible by fluorescence microscopy. We integrated the COX4-GFP gene at the nonessential *MFA2* locus (Michaelis and Herskowitz, 1988), which made fluorescence intensity uniform among cells and enabled efficient screening. After mutagenesis, individual cells with abnormal mitochondrial shape were hand-isolated using micropipettes (Fig. 1 A). This screening procedure allowed us to isolate individual mutant cells with interesting mitochondrial phenotypes from a large total population of cells.

Of ~72,000 cells screened, we isolated 20 mutants, which were classified into four categories (Fig. 1 B). Class I mutants (two isolates) contained one or two large, spherical mitochondria instead of the normal tubules seen in wild-type cells. Genetic crosses showed that both carried *mdm10* mutants (Sogo and Yaffe, 1994). The single class II mutant contained one or two oblong mitochondria collapsed to one side of the cell and was found to be defective in *SLM1*. *slm1* was previously identified as an *mmm1* synthetic-lethal mutant (Burgess et al., 1994; Burgess et al., manuscript in preparation). Class III mutants (three isolates) contained numerous mitochondrial fragments and

were shown to carry *fzo1* mutations. *FZO1* encodes a GTPase anchored in the mitochondrial outer membrane that is required for mitochondrial fusion (Hermann et al., 1998; Rapaport et al., 1998). Class IV mutants (14 isolates) exhibited a novel phenotype consisting of an interconnected network of mitochondrial tubules. In contrast to wild-type, which have 5–10 separate mitochondria per cell, class IV mutants appear to contain a single organelle. Because of their unique networked mitochondrial shape, these mutants were examined further.

Genetic crosses showed that our 14 class IV mutants comprised 8 recessive, 5 dominant and 1 semi-dominant mutations. Mapping studies showed that all 14 mutations were centromere linked (1.1 cM) and located on chromosome XII. We noted that *DNM1* (Gammie et al., 1995), a gene related to dynamin GTPase (Obar et al., 1990), maps to chromosome XII near the centromere and is required for mitochondrial shape (Otsuga et al., 1998). Using a *dnm1Δ* strain and a plasmid containing *DNM1* (kindly provided by J. Shaw), we found that all 14 class IV mutants carried *dnm1* alleles. These results were unexpected since mitochondrial shape in our mutants was strikingly different from previously seen in *dnm1* mutants, where mitochondria collapse to one side of the cell and form a single tubule (Otsuga et al., 1998).

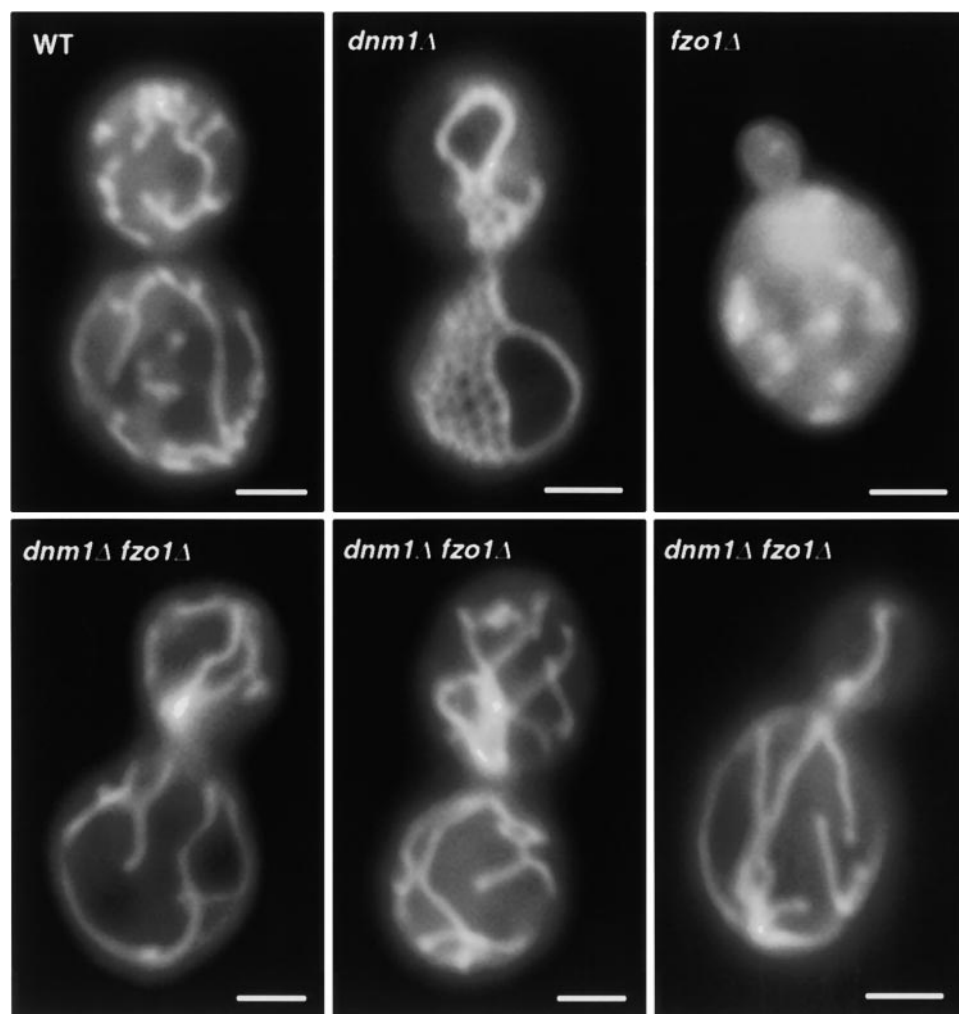


Figure 2. *dnm1Δ fzo1Δ* cells have normal-shaped mitochondria. Wild-type (BY4733) and isogenic deletion strains (*dnm1Δ*, *fzo1Δ*, and *dnm1Δ fzo1Δ*) expressing COX4-GFP (pHS12), were grown in YPGal to log phase and examined by fluorescence microscopy. Bars, 2 μ m.

A complete disruption of *DNM1* coding sequences was constructed, and examined for mitochondrial shape (Fig. 1 C). ~90% of *dnm1Δ* cells showed a single highly branched mitochondrial network. ~10% of *dnm1Δ* cells displayed a single mitochondrial tubule localized to one side of the cell, similar to that seen earlier (Otsuga et al., 1998). The mitochondrial shape was not dramatically altered by growth conditions (not shown). Mitochondria in *dnm1* mutants were efficiently segregated during cell division (Figs. 1 B and 2). Small daughter buds often contained a single mitochondrial tubule without branches, while larger buds had small networks. Most mitochondria were continuous from mother cells to buds, and separate mitochondria were only seen after the two cells separated. Our results strongly suggest that *dnm1* mutants are defective in mitochondrial division. We speculate that mitochondria in *dnm1* mutants may be divided indirectly, perhaps by cytokinesis. The yeast cell division machinery is clearly robust enough for the job, since nuclei are efficiently severed by cytokinesis in *S. pombe cut* mutants (Uzawa et al., 1990).

In yeast, mitochondria are very dynamic, fusing or dividing on average every two minutes (Nunnari et al., 1997). Thus there appears to be an equilibrium between fusion and division. Supporting this idea, when *FZO1*, a gene required for mitochondrial fusion, is defective, mitochondria fragment due to continued fission of the organelle (Hermann et al., 1998; Rapaport et al., 1998). We hypothesized that if mitochondrial division were blocked, cells would have fewer (larger) organelles. Our working model, based on the morphology of *dnm1* mutants, is that Dnm1p is required for mitochondrial division. To test this hypothesis, we constructed double mutants containing both *dnm1Δ* and *fzo1Δ* by genetic crosses. We found that normal mitochondrial shape was restored (Fig. 2). ~85% of double mutants contained multiply-branched, tubular mitochondria very similar to those seen in wild-type cells (Table I). This was in marked contrast to *dnm1Δ* mutants, which usually had a single organelle, and *fzo1Δ* mutants, with numerous mitochondrial fragments (Fig. 2; Hermann et al., 1998; Rapaport et al., 1998). Mitochondria in *dnm1Δ fzo1Δ* cells were not always completely normal; the tu-

bules tended to be longer and more curved than in wild-type cells, and occasionally formed bundles. Nonetheless, our observations suggest that excess mitochondrial division in *fzo1Δ* cells is suppressed by inactivating *DNM1*, and that excess mitochondrial fusion in *dnm1Δ* cells is rescued by *fzo1Δ*. We propose that division, which requires Dnm1p, and fusion, controlled by Fzo1p, have antagonistic effects on mitochondrial shape and number. Our results also suggest that mitochondrial tubule formation occurs by a mechanism independent of fusion and division.

Interestingly, mitochondrial shape and number in *dnm1Δ fzo1Δ* cells was dependent upon the order of gene disruption. When cells were first disrupted for *FZO1* and subsequently for *DNM1* (Table I, *fzo1Δ→dnm1Δ*), ~40% of cells carried mitochondrial fragments similar to those seen in *fzo1Δ* single mutants. In contrast, when cells were first disrupted for *DNM1* and then for *FZO1* (Table I, *dnm1Δ→fzo1Δ*), ~30% of cells displayed a mitochondrial network like that seen in *dnm1Δ* cells. Our results indicate that the mitochondrial networks found in *dnm1Δ* mutants

Table I. Mitochondrial Morphology in *dnm1Δfzo1Δ* Cells Created by Consecutive Gene Disruption or Genetic Cross

Mitochondrial morphology	<i>dnm1Δfzo1Δ</i> Cells created by consecutive gene disruption*		<i>dnm1Δfzo1Δ</i> Cells created by cross [‡]
	<i>fzo1Δ→dnm1Δ</i>	<i>dnm1Δ→fzo1Δ</i>	
	%	%	%
Tubules	50.0 ± 7.5	60.1 ± 4.7	84.7 ± 3.4
Networks	0.3 ± 0.7	30.6 ± 3.6	0.3 ± 0.6
Fragments	39.9 ± 5.2	0 ± 0	0 ± 0
Other [§]	9.8 ± 3.3	9.3 ± 3.1	14.9 ± 2.9

*Double mutants were generated by disrupting *FZO1* in *dnm1Δ* cells (*dnm1Δ→fzo1Δ*) or by disrupting *DNM1* in *fzo1Δ* cells (*fzo1Δ→dnm1Δ*). Cells were grown in YPGal, stained with 1 μg/ml DiOC₆, and examined for mitochondrial shape (tubules, networks, and fragments) by fluorescence microscopy.

[‡]*dnm1Δfzo1Δ* mutants were generated by crossing *dnm1Δ* to *fzo1Δ* cells (see Materials and Methods).

[§]Other indicated disorganized mitochondrial aggregates. The results were presented as the mean ± SD. At least 300 cells were scored in each experiment.

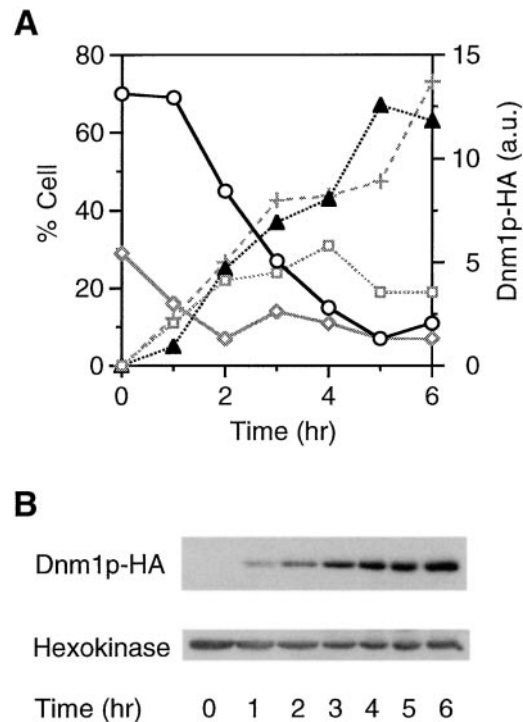


Figure 3. Expression of Dnm1p causes fragmentation of mitochondria in *dnm1Δ fzo1Δ* cells. *dnm1Δ fzo1Δ* cells carrying pCOX4-GFP (pHS12) and pGAL1-DNM1-HA (pHS15) were pregrown in raffinose medium, centrifuged and resuspended to an OD₆₀₀ of 0.2 in galactose medium (SGS) to induce Dnm1p-HA expression. Cells were examined for mitochondrial shape ($n = 100$) or used to prepare total protein at the indicated timepoints. (A) Mitochondrial shape was classified into the following four groups: tubules (○), partially fragmented tubules (□), fragments (▲), and other (◇). (B) Total protein was extracted as described (Yaffe and Schatz, 1984) and subjected to Western blot analysis using antibodies to the HA epitope (Field et al., 1988), or hexokinase (Davis, A., unpublished data) followed by chemiluminescence (Pierce). Relative amounts of Dnm1p-HA (+) were quantitated and plotted in A.

persist in the absence of fusion activity, and fragments formed in the *fzo1Δ* mutant persist in the absence of fission activity. We also found tubular mitochondria in many of the double mutant cells formed by consecutive gene disruption (~50% for *fzo1Δ*→*dnm1Δ*; ~60% for *dnm1Δ*→*fzo1Δ*). These results further indicate that mitochondrial tubules form in the absence of division and fusion. It is not clear why *dnm1Δ fzo1Δ* double mutants generated by crossing a *dnm1Δ* cell to a *fzo1Δ* cell contained mostly (>80%) tubular mitochondria and essentially no mitochondrial networks or fragments (Table I). During germination and growth of a *dnm1Δ fzo1Δ* spore, it is possible that cells are simultaneously depleted of Dnm1p and Fzo1p, leading to the formation of tubules, but not networks or fragments.

To further test the role of Dnm1p in division, we induced Dnm1p expression in *dnm1Δ fzo1Δ* cells and observed its effect on mitochondria. Dnm1p was fused to the HA epitope (Dnm1p-HA) (Field et al., 1988) and expressed under the galactose-inducible *GAL1* promoter (Nigro et al., 1992). Our pGAL1-DNM1-HA rescued the *dnm1Δ* phenotype on galactose medium (not shown). When *dnm1Δ fzo1Δ* cells containing pGAL1-DNM1-HA were grown in the absence of galactose, no Dnm1p-HA was detected (Fig. 3 B) and ~70% of cells displayed the tubular mitochondria typical of *dnm1Δ fzo1Δ* mutants (Fig. 3 A). Upon transfer to galactose medium, Dnm1p-HA levels gradually increased, while the level of hexokinase, a control protein, remained constant (Fig. 3 B). Concomitant with the accumulation of Dnm1p-HA, mitochondrial shape changed dramatically (Fig. 3 A). The number of cells with tubular mitochondria decreased, and those with fragmented mitochondria increased. By 5 h, ~65% of the cells contained completely fragmented mitochondria. At intermediate times (2 h) after inducing Dnm1p-HA, cells contained partially fragmented tubules, and many mitochondrial tubules were adjacent to small fragments. Our

results clearly show that the division of mitochondria in *dnm1Δ fzo1Δ* cells coincides with the expression of Dnm1p.

Further supporting a role for Dnm1p in mitochondrial fission, we found that the Dnm1 protein was preferentially localized to sites of mitochondrial division. We constructed a fusion between Dnm1p and the green fluorescent protein (GFP). Consistent with previous results (Otsuga et al., 1998), we found that much of Dnm1p-GFP was associated with mitochondria in punctate structures (Fig. 4 A). In cells that were constitutively expressing Dnm1p-GFP, it was difficult to determine the precise location of Dnm1p because of the complex morphology of the mitochondria and the large number of Dnm1p-GFP dots. To simplify our analyses, we induced the expression of Dnm1p-GFP in the *dnm1Δ fzo1Δ* mutant and examined cells at early times after induction. We found a tight correlation between the appearance of Dnm1p-GFP and fragmentation of mitochondria. Two representative cells are shown in Fig. 4, B and C; both cells contained two Dnm1p-GFP dots, one of which was located at the end of a tubule, the other appeared to be reside near a constricted region of the mitochondrion. After analysis of additional cells, we found that Dnm1p-GFP was localized to ends of mitochondrial fragments much more frequently (>60%) than predicted if Dnm1p-GFP was randomly distributed on mitochondria (~11%). These results suggest that Dnm1p acts at the site of mitochondrial fission. We note that Dnm1p-GFP is not exclusively found at the ends of mitochondria. We surmise that Dnm1p on the sides of the tubules may mark future sites of division, or represent Dnm1p-containing complexes that have diffused away from the end of the tubule. More definitive experiments (e.g., time-lapse videomicroscopy) to determine the role of Dnm1p in fission are in progress.

The relatively normal mitochondria seen in *dnm1Δ fzo1Δ* mutants could be explained by a restoration of fu-

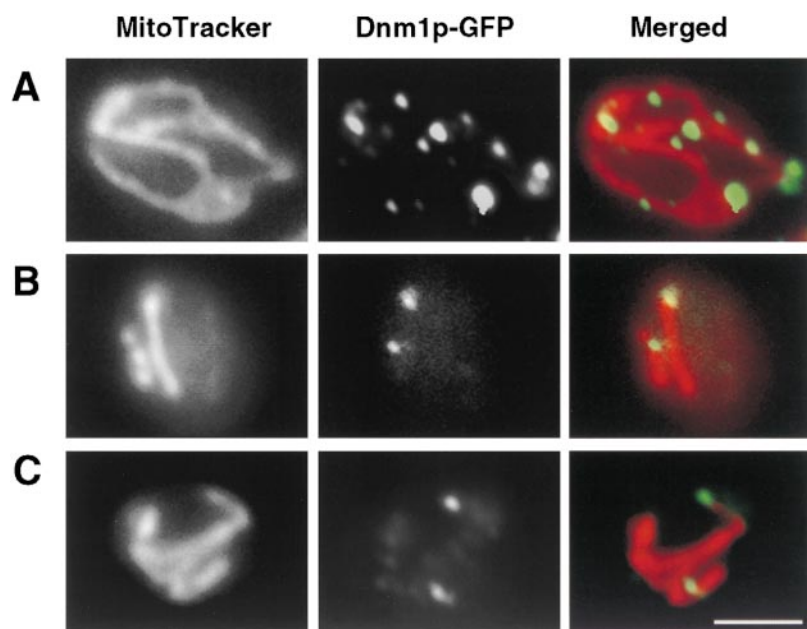


Figure 4. A Dnm1p-GFP preferentially localizes to site of mitochondrial division. (A) *dnm1Δ* strain YHS19 was transformed with pHS20 expressing Dnm1p-GFP. Cells were grown in SGal medium, labeled with 0.1 μ M MitoTracker Red CMXRos (Molecular Probes) and then examined under the fluorescence microscope. Merged images taken in the red (MitoTracker) and green (GFP) channels are shown. (B and C) *dnm1Δ fzo1Δ* diploid cells carrying pGAL1-DNM1-GFP were pregrown in YPglycerol/ethanol medium, centrifuged and grown in galactose medium (SGS) for 1–2 h. Cells were then stained with MitoTracker and examined for mitochondrial localization of Dnm1p-GFP. Two representative cells are shown. Bar, 3 μ m.

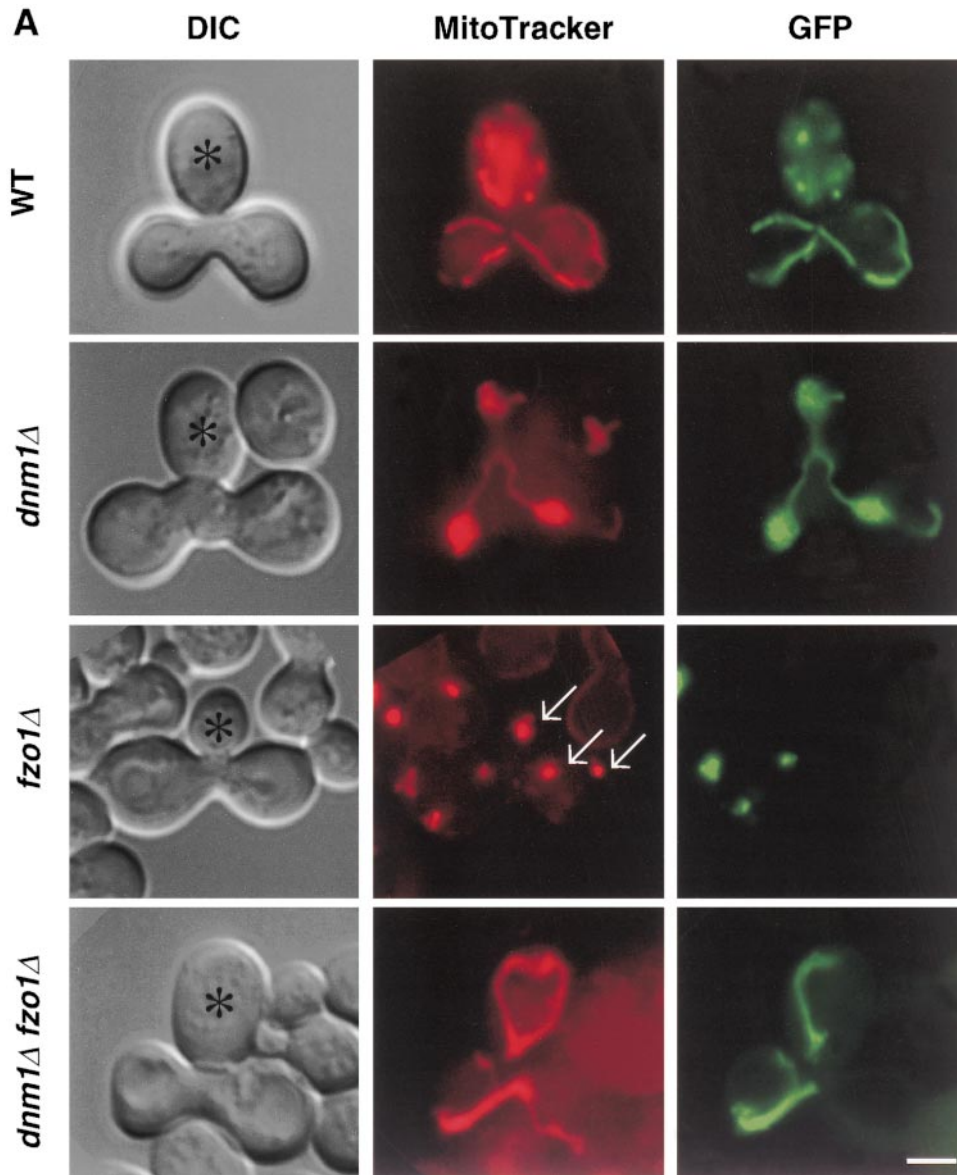
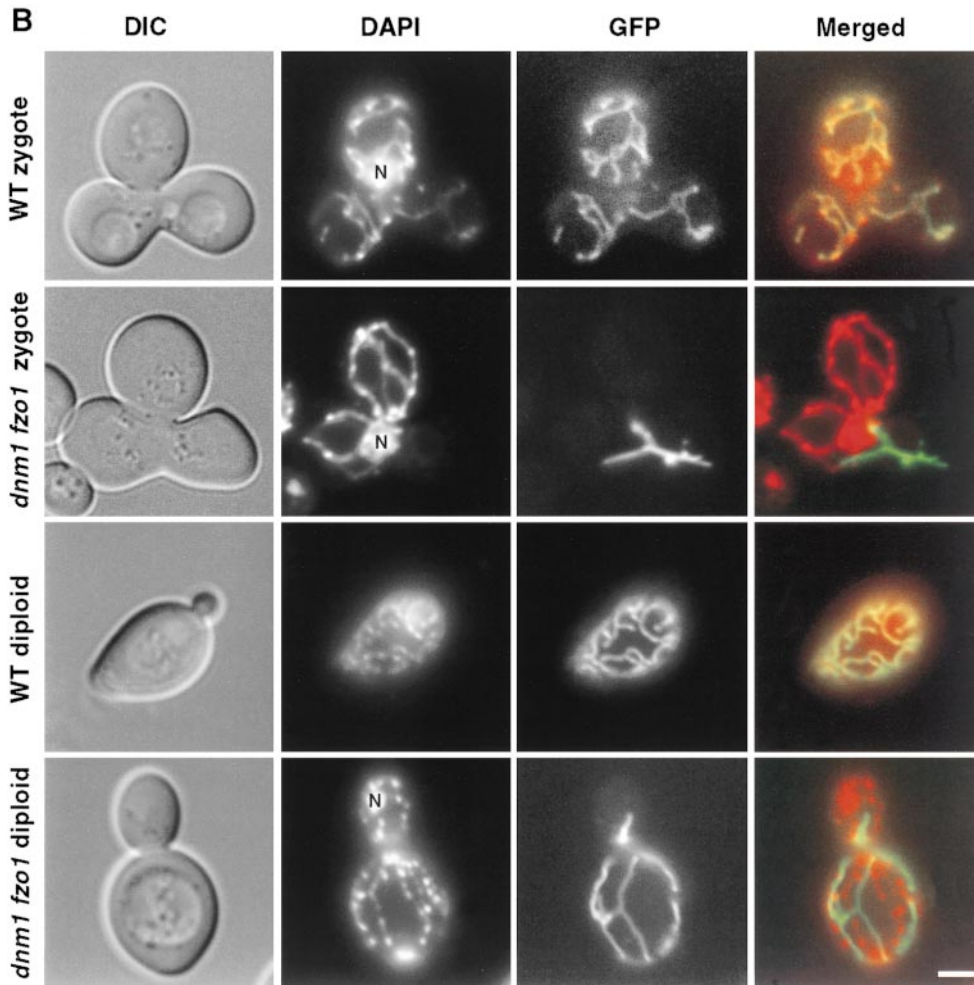


Figure 5 (continues on facing page).

sion activity; for example, if Dnm1p were an inhibitor of mitochondrial fusion. To test this possibility, we monitored mitochondrial fusion during mating (Nunnari et al., 1997; Okamoto et al., 1998). Mitochondria were visualized in one parent, by the galactose-induced expression of a matrix-targeted GFP (CS1-GFP) on plasmid pCLbGFP (Okamoto et al., 1998). *MAT α* cells containing pCLbGFP were pregrown in galactose medium to induce CS1-GFP expression, then transferred to glucose to inhibit further synthesis. *MAT α* cells were then mixed with *MAT α* cells, which did not carry pCLbGFP, and allowed to mate on glucose medium. Mitochondria were visualized in zygotes using MitoTracker. If mitochondrial fusion occurred, GFP and MitoTracker fluorescence would completely overlap, because the matrix-localized CS1-GFP from the *MAT α* mitochondria diffused into the mitochondrial matrix of the *MAT α* cell. If no fusion occurred, GFP-labeled mitochondria would be seen in only one half of the zygote.

Zygotes formed by two wild-type cells, or two *dnm1 Δ* mutants, exhibited efficient mitochondrial fusion, with GFP fluorescence and MitoTracker overlapping in all mitochondria (Fig. 4 A). In contrast, fusion was defective in *fzo1 Δ* mutants, consistent with previous observations (Hermann et al., 1998). Mitochondrial fragments tended to aggregate in *fzo1 Δ* cells and individual fragments were difficult to distinguish. Nonetheless, in matings between two *fzo1 Δ* cells, MitoTracker showed clusters of fragmented mitochondria in the zygote and diploid bud, but we detected GFP fluorescence in only half of the mitochondrial clusters. Like *fzo1 Δ* mutants, *dnm1 Δ fzo1 Δ* double mutants failed to fuse their mitochondria. Although mitochondria in *dnm1 Δ fzo1 Δ /dnm1 Δ fzo1 Δ* diploid cells had normal shape, only half of the organelles contained GFP. Our results indicate that *dnm1 Δ fzo1 Δ* cells are defective in mitochondrial fusion.

To eliminate the possibility that low, basal levels of fu-



tants is shown. Fluorescence (GFP or DAPI), differential interference contrast (DIC) and merged images are shown. Mating mixtures were also incubated for an additional 24 h at 30°C on YPD, and representative diploids are shown. N indicates nuclear DNA staining. Bar, 3 μ m.

sion occur in *dnm1Δ fzo1Δ* cells, we used a more sensitive fusion assay using the matrix markers, CS1-GFP and mitochondrial DNA (mtDNA; Okamoto et al., 1998). 4',6-diamidino-2-phenylindole (DAPI) stained mtDNA was a more stable probe compared with MitoTracker, allowing us to examine cells for longer times following the initial mating event. *MAT α* cells, which lacked mtDNA and carried pCLbGFP were mated to *MAT α* cells, which contained mtDNA, but not the plasmid (Fig. 5 B). The DAPI and GFP fluorescence overlapped in all the mitochondrial tubules in wild-type zygotes (52 zygotes examined). When 500 *dnm1Δ fzo1Δ* zygotes were examined, we found no overlap between DAPI and GFP. The fusion activity in *dnm1Δ fzo1Δ* mutants is therefore at least 500-fold less than that in wild-type cells. Even after the zygotes were allowed to grow and divide, we found no fusion in the mutant cells (Fig. 5 B). When 100 *dnm1Δ fzo1Δ/dnm1Δ fzo1Δ* diploid cells were examined 24 h after mating, none contained an overlap between GFP and DAPI, whereas a complete GFP and DAPI overlap was seen in 43 wild-type diploids. *dnm1Δ fzo1Δ* cells clearly lack significant mitochondrial fusion activity. Our results above also suggest

that *dnm1Δ fzo1Δ* cells lack fission activity. We therefore propose that in cells lacking Fzo1p and Dnm1p, mitochondrial tubule formation occurs by a mechanism independent of fusion and division, such as growth from the ends of preexisting organelles.

Dynamin has been proposed to work as a mechanochemical enzyme that 'pinches off' plasma membrane invaginations, forming intracellular vesicles (Takei et al., 1995). Supporting this idea, dynamin self-assembles into spiral-like structures (Hinshaw and Schmid, 1995) which can sever artificial membranes in vitro (Sweitzer and Hinshaw, 1998). It is also possible that dynamin plays a regulatory, instead of an enzymatic, function in membrane scission (Sever et al., 1999). Future studies are clearly needed to determine the precise mechanism that Dnm1p plays in mitochondrial division.

We especially thank J. Shaw for generous gifts of strains and plasmids. We also thank J. Holder, O. Kerscher, S. Michaelis, J. Boeke, A. Aiken, A. Davis, R. Butow, K. Okamoto, D. Murphy, R. Bustos, C. Machamer, and T. Kai for reagents, equipment and technical advice. We thank C. Machamer, K. Wilson, and the members of the Jensen lab for valuable comments on the manuscript.

Figure 5. *dnm1Δ fzo1Δ* cells are defective in mitochondrial fusion. (A) *MAT α* cells that express CS1-GFP from the *GAL1* promoter of pCLbGFP were grown in galactose-containing medium (SGS). *MAT α* cells lacking the plasmid were grown in glucose medium (YPD). *MAT α* and α cells carrying the indicated genotypes were mated on YPD for 3.5 h, and then stained with 0.1 μ M MitoTracker. The distribution of MitoTracker and GFP in representative zygotes containing a medial bud (asterisks) are shown. Arrows indicate three clusters of mitochondria lacking CS1-GFP in *fzo1Δ* zygotes. (B) Wild-type and *dnm1Δ fzo1Δ MAT α* cells were treated with ethidium bromide to induce loss of mtDNA (Fox et al., 1991), transformed with pCLbGFP, and then grown in galactose-containing medium (SGS). Wild-type and *dnm1Δ fzo1Δ MAT α* cells containing mtDNA, but lacking the plasmid, were grown in YPD. Cells were mated on YPD and stained with 0.5 μ g/ml 4',6-diamidino-2-phenylindole (DAPI; Molecular Probes). A representative zygote formed by mating between wild-type cells or between *dnm1Δ fzo1Δ* mu-

This work was supported by a PHS grant (R01-GM54021) to R.E. Jensen and a JSPS fellowship to H. Sesaki.

Submitted: 27 July 1999

Revised: 1 October 1999

Accepted: 4 October 1999

References

- Adams, A., D. Gottschling, C. Kaiser, and T. Stearns. 1997. *Methods in Yeast Genetics*. Cold Spring Harbor Laboratory Press, Plainview, NY.
- Bereiter-Hahn, J., and M. Voth. 1994. Dynamics of mitochondria in living cells: shape changes, dislocations, fusion, and fission of mitochondria. *Microsc. Res. Tech.* 27:198–219.
- Brachmann, C.B., A. Davies, C.G.J., E. Caputo, J. Li, P. Hieter, and J.D. Boeke. 1998. Designer deletion strains from *Saccharomyces cerevisiae* 288C: a useful set of strains and plasmids for PCR-mediated gene disruption and other applications. *Yeast* 14:115–132.
- Burgess, S.M., M. Delannoy, and R.E. Jensen. 1994. *MMM1* encodes a mitochondrial outer membrane protein essential for establishing and maintaining the structure of yeast mitochondria. *J. Cell Biol.* 126:1375–1391.
- Field, J., J. Nikawa, D. Broek, B. MacDonald, L. Rodgers, I.A. Wilson, R.A. Lerner, and M. Wigler. 1988. Purification of a RAS-responsive adenyl cyclase complex from *Saccharomyces cerevisiae* by use of an epitope addition method. *Mol. Cell Biol.* 8:2159–2165.
- Fox, T.D., L.S. Folley, J.J. Mulero, T.W. McMullin, P.E. Thorsness, L.O. Hedlin, and M.C. Costanzo. 1991. Analysis and manipulation of yeast mitochondrial genes. *Methods Enzymol.* 194:149–165.
- Gammie, A.E., L.J. Kurihara, R.B. Vallee, and M.D. Rose. 1995. DNM1, a dynamin-related gene, participates in endosomal trafficking in yeast. *J. Cell Biol.* 130:553–566.
- Hales, K.G., and M.T. Fuller. 1997. Developmentally regulated mitochondrial fusion mediated by a conserved, novel, predicted GTPase. *Cell* 90:121–129.
- Hermann, G.J., J.W. Thatcher, J.P. Mills, K.G. Hales, M.T. Fuller, J. Nunnari, and J.M. Shaw. 1998. Mitochondrial fusion in yeast requires the transmembrane GTPase Fzo1p. *J. Cell Biol.* 143:359–373.
- Hinshaw, J.E., and S.L. Schmid. 1995. Dynamin self-assembles into rings suggesting a mechanism for coated vesicle budding. *Nature* 374:190–192.
- Kawano, S., H. Takano, and T. Kuroiwa. 1995. Sexuality of mitochondria: fusion, recombination, and plasmids. *Int. Rev. Cytol.* 161:49–110.
- Lorenz, M.C., R.S. Muir, E. Lim, J. McElver, S.C. Weber, and J. Heitman. 1995. Gene disruption with PCR products in *Saccharomyces cerevisiae*. *Gene* 158:113–117.
- Michaelis, S., and I. Herskowitz. 1988. The a-factor pheromone of *Saccharomyces cerevisiae* is essential for mating. *Mol. Cell Biol.* 8:1309–1318.
- Miyakawa, I., H. Aoi, N. Sando, and T. Kuroiwa. 1984. Fluorescence microscopic studies of mitochondrial nucleoids during meiosis and sporulation in the yeast, *Saccharomyces cerevisiae*. *J. Cell Sci.* 66:21–38.
- Nigro, J.M., R. Sikorski, S.I. Reed, and B. Vogelstein. 1992. Human p53 and *CDC2Hs* genes combine to inhibit the proliferation of *Saccharomyces cerevisiae*. *Mol. Cell Biol.* 12:1357–1365.
- Nunnari, J., W.F. Marshall, A. Straight, A. Murray, J.W. Sedat, and P. Walter. 1997. Mitochondrial transmission during mating in *Saccharomyces cerevisiae* is determined by mitochondrial fusion and fission and the intramitochondrial segregation of mitochondrial DNA. *Mol. Biol. Cell* 8:1233–1242.
- Obar, R.A., C.A. Collins, J.A. Hammarback, H.S. Shpetner, and R.B. Vallee. 1990. Molecular cloning of the microtubule-associated mechanochemical enzyme dynamin reveals homology with a new family of GTP-binding proteins. *Nature* 347:256–261.
- Okamoto, K., P.S. Perlman, and R.A. Butow. 1998. The sorting of mitochondrial DNA and mitochondrial proteins in zygotes: preferential transmission of mitochondrial DNA to the medial bud. *J. Cell Biol.* 142:613–623.
- Oldenburg, K.R., K.T. Vo, S. Michaelis, and C. Paddon. 1997. Recombination-mediated PCR-directed plasmid construction in vivo in yeast. *Nucleic Acids Res.* 25:451–452.
- Otsuga, D., B.R. Keegan, E. Brisch, J.W. Thatcher, G.J. Hermann, W. Bleazard, and J.M. Shaw. 1998. The dynamin-related GTPase, Dnm1p, controls mitochondrial morphology in yeast. *J. Cell Biol.* 143:333–349.
- Pon, L., and G. Schatz. 1991. Biogenesis of yeast mitochondria. In *The Molecular Biology of the Yeast Saccharomyces*. J.R. Broach, J.R. Pringle, and E.W. Jones, editors. Cold Spring Harbor Laboratory Press, New York. 333–406.
- Rapaport, D., M. Brunner, W. Neupert, and B. Westermann. 1998. Fzo1p is a mitochondrial outer membrane protein essential for the biogenesis of functional mitochondria in *Saccharomyces cerevisiae*. *J. Biol. Chem.* 273:20150–20155.
- Sever, S., A.B. Muhlberg, and S.L. Schmid. 1999. Impairment of dynamin's GAP domain stimulates receptor-mediated endocytosis. *Nature* 398:481–486.
- Sikorski, R., and P. Hieter. 1989. A system of shuttle vectors and host strains designed for efficient manipulation of DNA in *Saccharomyces cerevisiae*. *Genetics* 122:19–28.
- Sogo, L.F., and M.P. Yaffe. 1994. Regulation of mitochondrial morphology and inheritance by Mdm10p, a protein of the mitochondrial outer membrane. *J. Cell Biol.* 126:1361–1373.
- Stevens, B.J. 1977. Variation in number and volume of the mitochondria in yeast according to growth conditions. A study based on serial sectioning and computer graphics reconstitution. *Biol. Cell* 28:37–56.
- Sweitzer, S.M., and J.E. Hinshaw. 1998. Dynamin undergoes a GTP-dependent conformational change causing vesiculation. *Cell* 93:1021–1029.
- Takei, K., P.S. McPherson, S.L. Schmid, and P. De Camilli. 1995. Tubular membrane invaginations coated by dynamin rings are induced by GTP-gamma S in nerve terminals. *Nature* 374:186–190.
- Tyler, D. 1992. *The Mitochondrion*. VCH Publishers, New York.
- Uzawa, S., I. Samejima, T. Hirano, K. Tanaka, and M. Yanagida. 1990. The fission yeast cut1+ gene regulates spindle pole body duplication and has homology to the budding yeast ESP1 gene. *Cell* 62:913–925.
- Yaffe, M.P., and G. Schatz. 1984. Two nuclear mutations that block mitochondrial protein import in yeast. *Proc. Natl. Acad. Sci. USA* 81:4819–4823.